INCREMENTS IN AEROFOIL LIFT COEFFICIENT AT ZERO ANGLE OF ATTACK AND IN MAXIMUM LIFT COEFFICIENT DUE TO DEPLOYMENT OF A PLAIN TRAILING-EDGE FLAP, WITH OR WITHOUT A LEADING-EDGE HIGH-LIFT DEVICE, AT LOW SPEEDS

1. NOTATION AND UNITS

		SI	*British*
A	parameter in equation for T, Equation (4.14)		
a_t	theoretical rate of change of lift coefficient with trailing-edge flap deflection, Equation (4.2)	rad^{-1}	rad^{-1}
B	parameter in equation for T, Equation (4.15)		
C	parameter in equation for T, Equation (4.16)		
C_{Lm}	maximum lift coefficient of aerofoil with high-lift devices deployed, based on c		
C_{L0}	lift coefficient at zero angle of attack for aerofoil with high-lift devices deployed, based on c		
ΔC_{Lm}	increment in maximum lift coefficient due to deployment of high-lift devices, based on c, Equation (3.2)		
ΔC_{Lml}	increment in maximum lift coefficient due to deployment of leading-edge high-lift device, based on c, Equation (3.2)		
ΔC_{Lmt}	increment in maximum lift coefficient due to deployment of trailing-edge flap, based on c, Equation (3.5)		
$\Delta C'_{Lmt}$	increment in maximum lift coefficient due to deployment of trailing-edge flap, based on c', Equation (4.8), at datum Reynolds number $R_c = 3.5 \times 10^6$		
ΔC_{L0}	increment in lift coefficient at zero angle of attack due to deployment of high-lift devices, based on c, Equation (3.1)		
ΔC_{L0l}	increment in lift coefficient at zero angle of attack due to deployment of leading-edge high-lift device, based on c, Equation (3.1)		
ΔC_{L0t}	increment in lift coefficient at zero angle of attack due to deployment of trailing-edge flap, based on c, Equation (3.4)		
$\Delta C'_{L0t}$	increment in lift coefficient at zero angle of attack due to deployment of trailing-edge flap, based on c', Equation (4.5)		
c	basic (plain) aerofoil chord (*i.e.* chord with high-lift devices undeployed), see Sketch 4.1	m	ft

Issued December 1994

c'	extended aerofoil chord (*i.e.* chord with high-lift devices deployed), see Sketch 4.1	m	ft
c_{el}	effective chord of leading-edge device, see Item No. 94027	m	ft
c_t	chord of trailing-edge flap, see Sketch 4.1	m	ft
Δc_l	chord extension due to deployment of leading-edge device, see Sketch 4.1	m	ft
Δc_t	chord extension due to deployment of trailing-edge flap, Equation (4.6); $\Delta c_t = 0$ for plain flap	m	ft
F_R	factor for effect of Reynolds number on ΔC_{Lml} and ΔC_{Lmt}, Equation (3.3)		
J_p	correlation factor (efficiency factor) for plain flap in Equation (4.5), Figure 1		
K_G	correlation factor for aerofoil geometry in Equation (4.8), Equation (4.9)		
K_t	correlation factor for flap deflection in Equation (4.8); $K_t = 0.8$ for plain flap		
M	free-stream Mach number		
R_c	Reynolds number based on free-stream conditions and aerofoil chord c		
T	theoretical value of $\Delta C'_{Lmt}/\Delta C'_{L0t}$, Equation (4.11) or (4.13) or Figure 2		
t	maximum thickness of aerofoil	m	ft
x'_s	chordwise location of boundary-layer separation measured from leading edge of extended chord, Equation (4.12)	m	ft
δ_t, δ_t°	deflection of trailing-edge flap, positive trailing edge down, see Sketch 4.1	rad, deg	rad, deg
θ_s	angular parameter related to location of separation, Equation (4.12)	rad	rad
θ_t	angular parameter related to trailing-edge flap chord, Equation (4.3)	rad	rad
ρ_l	leading-edge radius of basic (plain) aerofoil, see Sketch 4.1	m	ft
ϕ_t°	angle between aerofoil datum and tangent to upper surface at trailing edge, see Sketch 4.1	deg	deg

Subscripts

$( )_{expt}$ denotes experimental value

$( )_{pred}$ denotes predicted value

2. INTRODUCTION

2.1 Scope of the Item

This Item provides semi-empirical methods for estimating the incremental effects on aerofoil lift at zero angle of attack and on maximum lift due to the deployment of plain trailing-edge flaps, with or without the deployment of leading-edge high-lift devices, at low speeds.

Section 3 summarises the equations relating the contributions to the total lift increments at zero angle of attack and at maximum lift arising from the deployment of leading-edge high-lift devices and trailing-edge flaps. The contributions from leading-edge high-lift devices are obtainable from Derivation 8. Section 4 presents methods whereby the contributions from plain trailing-edge flaps are obtained.

Section 5 concerns applicability and accuracy, Section 6 gives the Derivation and References and Section 7 presents two detailed examples illustrating the use of the methods.

2.2 Application of Data to Calculation of Total Lift Coefficient Values C_{L0} and C_{Lm}

In order to use the data obtained from the present Item in the wider context in which the total lift coefficient at zero angle of attack, C_{L0}, and at maximum lift, C_{Lm}, are required for an aerofoil with high-lift devices deployed, it is necessary to refer to Item No. 94026 (Reference 9). That Item acts as an introduction to, and a link between, the Items in the complete series dealing with the incremental effects of high-lift device deployment on aerofoil lift at zero angle of attack and on maximum lift. It describes how the incremental effects are summed and added to the contributions from the basic (*i.e.* plain) aerofoil to give the total values C_{L0} and C_{Lm}.

3. LIFT COEFFICIENT INCREMENTS ΔC_{L0} AND ΔC_{Lm}

The increments in the lift coefficient at zero angle of attack, ΔC_{L0}, and at maximum lift, ΔC_{Lm}, due to the deployment of a leading-edge high-lift device and a trailing-edge flap on an aerofoil are given by the sum of the individual increments, *i.e.*

$$\Delta C_{L0} = \Delta C_{L0l} + \Delta C_{L0t} \tag{3.1}$$

and

$$\Delta C_{Lm} = \Delta C_{Lml} + \Delta C_{Lmt}. \tag{3.2}$$

The increments in Equations (3.1) and (3.2) are based on the chord, c, of the basic aerofoil.

The values of ΔC_{L0l} and ΔC_{Lml} for various leading-edge high-lift devices are obtainable from Item No. 94027 (Derivation 8).

For correlation purposes it is more convenient to present the right-hand sides of Equations (3.1) and (3.2) in terms of increments based on the aerofoil extended chord c'. Also, whereas values of ΔC_{L0l} and ΔC_{L0t} can be taken to be independent of Reynolds number, values of ΔC_{Lml} and ΔC_{Lmt} are influenced by Reynolds number. Analysis of data in derivations 5 and 7 showed that if the increments in maximum lift coefficient were correlated at a datum Reynolds number, taken here as $R_c = 3.5 \times 10^6$ (see Section 5), then all the Reynolds number dependency could be allowed for through a factor F_R, given by

$$F_R = 0.153 \log_{10} R_c , \tag{3.3}$$

which is unity at the datum.

Therefore, the terms related to the trailing-edge flap on the right-hand sides of Equations (3.1) and (3.2) become

$$\Delta C_{L0t} = \frac{c'}{c} \Delta C'_{L0t} \tag{3.4}$$

and

$$\Delta C_{Lmt} = F_R \frac{c'}{c} \Delta C'_{Lmt} . \tag{3.5}$$

The values of $\Delta C'_{L0t}$ and $\Delta C'_{Lmt}$ in Equations (3.4) and (3.5) for plain trailing-edge flaps are determined by the methods of Section 4.

4. LIFT COEFFICIENT INCREMENTS $\Delta C'_{L0t}$ AND $\Delta C'_{Lmt}$

First approximations to the lift coefficient increments due to the deployment of trailing-edge flaps can be obtained from the theory for an equivalent thin hinged plate with empirical correlation factors to account for the geometry of practical aerofoils and flaps. To make some allowance for the effects of chord extension in the theory the flap chord ratio and the lift coefficient increments are based on the aerofoil extended chord. This approach was used in Derivation 6 and is the basis for the methods developed for this Item, see Sections 4.1 and 4.2.

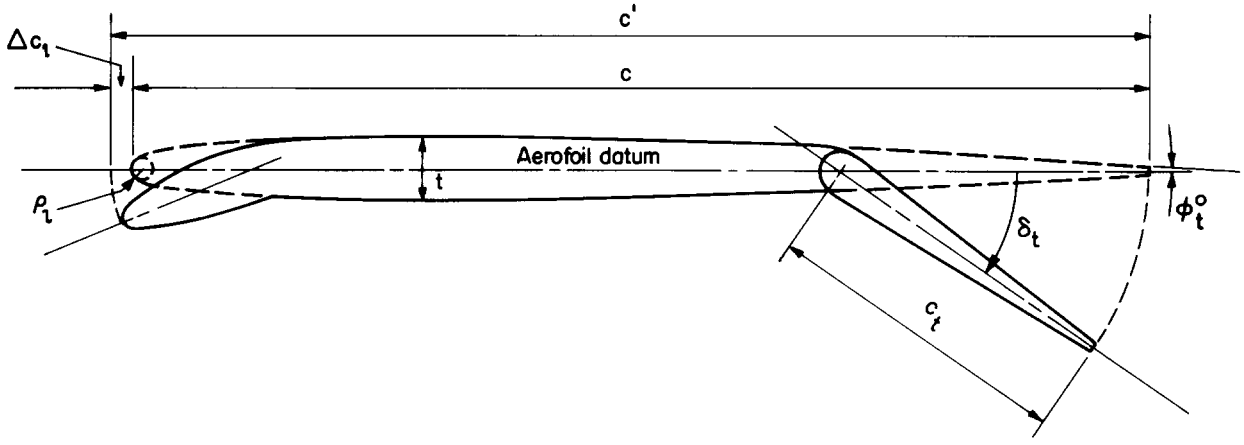

Sketch 4.1 Plain trailing-edge flap with typical leading-edge high-lift device (leading-edge droop)

4.1 Increment in Lift Coefficient at Zero Angle of Attack

The increment in lift coefficient at zero angle of attack due to the deployment of a plain trailing-edge flap is

$$\Delta C'_{L0t} = J_p a_t \delta_t \tag{4.1}$$

where J_p is an empirical correlation factor, (or efficiency factor) and a_t is the theoretical rate of change of lift coefficient with respect to the deflection δ_t, positive trailing edge down, at constant angle of attack, given by thin plate theory as

$$a_t = 2(\pi - \theta_t + \sin\theta_t) \tag{4.2}$$

where
$$\theta_t = \cos^{-1}(2c_t/c' - 1) \tag{4.3}$$

and
$$\sin\theta_t = [1 - (2c_t/c' - 1)^2]^{\frac{1}{2}}, \tag{4.4}$$

in which c_t is the chord of the plain flap.

Combination of Equations (4.1) to (4.4) gives

$$\boxed{\Delta C'_{L0t} = 2J_p\delta_t\{\pi - \cos^{-1}(2c_t/c' - 1) + [1 - (2c_t/c' - 1)^2]^{\frac{1}{2}}\}.} \tag{4.5}$$

The parameter J_p is given in Figure 1 as a function of the angle $(\delta_t^\circ + \phi_t^\circ)$, where ϕ_t° is the angle between the aerofoil datum and the tangent to the upper surface at the trailing edge, see Sketch 4.1.

When there is a deployed leading-edge high-lift device, the extended aerofoil chord c' in Equation (4.5) is given by

$$c' = c + \Delta c_l + \Delta c_t. \tag{4.6}$$

For a plain flap $\Delta c_t = 0$, so that

$$c' = c + \Delta c_l. \tag{4.7}$$

and the value of Δc_l for a variety of leading-edge high-lift devices is obtained from Item No. 94027.

The value of $\Delta C'_{L0t}$ is then used in Equation (3.4) to determine ΔC_{L0t}.

4.2 Increment in Maximum Lift Coefficient

The increment in maximum lift coefficient is given by

$$\boxed{\Delta C'_{Lmt} = K_G K_t T \Delta C'_{L0t}.} \tag{4.8}$$

The parameter K_G is an empirical correlation factor for aerofoil geometry, based on that given in Derivation 6, and is represented by

$$K_G = 1.225 + 4.525\rho_l/t\,. \tag{4.9}$$

The parameter K_t is an empirical correlation factor, generally dependent on flap deflection, but which for plain flaps can be taken as a constant,

$$K_t = 0.8. \tag{4.10}$$

The parameter T is the theoretical value of the ratio $\Delta C'_{Lmt}/\Delta C'_{L0t}$ derived from thin aerofoil theory on the basis of Derivation 6 as

$$T = 1 - \frac{\pi - \theta_t}{\pi - \theta_t + \sin\theta_t}\left[1 + \frac{\log_e\left|\sin ½(\theta_t + \theta_s)/\sin ½(\theta_t - \theta_s)\right|}{(\pi - \theta_t)\cot ½\theta_s}\right], \tag{4.11}$$

where

$$\theta_s = \cos^{-1}(1 - 2x'_s/c'), \tag{4.12}$$

and x'_s is the distance of the position of boundary-layer separation from the leading edge of the extended chord.

By means of Equations (4.3), (4.4) and (4.12), Equation (4.11) can be manipulated into the form

$$T = 1 - \frac{1}{1+A}\left[1 + B\log_e\left|\frac{1 + C^{½}}{1 - C^{½}}\right|\right], \tag{4.13}$$

where

$$A = \frac{2[(c_t/c')(1 - c_t/c')]^{½}}{\pi - \cos^{-1}(2c_t/c' - 1)} \tag{4.14}$$

$$B = \frac{[(x'_s/c')/(1 - x'_s/c')]^{½}}{\pi - \cos^{-1}(2c_t/c' - 1)} \tag{4.15}$$

and

$$C = \left(\frac{c_t/c'}{1 - c_t/c'}\right)\left(\frac{x'_s/c'}{1 - x'_s/c'}\right). \tag{4.16}$$

Note that $A \to 1$ as $c_t/c' \to 0$. Also $B \to 0.5$ and $C \to 0$ as $x'_s/c' \to 0$ and $c_t/c' \to 0$.

For aerofoils with smooth leading edges and a deployed trailing-edge flap it is assumed that $x'_s/c' = 0$. As noted in Reference 9, the additional deployment of a leading-edge high-lift device interferes to some extent with the flow field around the trailing-edge flap in the region of maximum lift. The parameter T can be used as a means of accounting for the effect of that interference on $\Delta C'_{Lmt}$ by means of a judicious choice of x'_s/c'. The magnitude of the interference appears to depend on the trailing-edge flap type, but is usually fairly small. The limited data (Derivation 4) show that $x'_s/c' = ½\ c_{el}/c'$ gives the best correlation for plain flaps. Information concerning the effective chord, c_{el}, for a variety of leading-edge devices is given in Table 4.1 of Item No. 94027. The variation of T with c_t/c' and x'_s/c', determined from Equation (4.13), is given in Figure 2.

The value of $\Delta C'_{L0t}$ in Equation (4.8) is determined using Equation (4.5) in Section 4.1. That section also provides information concerning the evaluation of c' when a leading-edge high-lift device is deployed. Then, with the resulting value of $\Delta C'_{Lmt}$ the value of ΔC_{Lmt} is determined from Equation (3.5) with F_R given by Equation (3.3).

5. APPLICABILITY AND ACCURACY

5.1 Applicability

Methods are given in this Item for estimating the increments in aerofoil lift coefficient at zero angle of attack and in maximum lift coefficient due to the deployment of plain trailing-edge flaps with or without the deployment of leading-edge high-lift devices.

The measured data, used in the analysis, were obtained from Derivations 1 to 4 and covered the ranges of the various correlation parameters given in Table 5.1. Although data (Derivation 4) were available for plain trailing-edge flaps in combination with only one type of leading-edge high lift device (plain leading-edge flap) it is anticipated that the methods will apply to any of the types of leading-edge device treated in Item No. 94027.

The value $R_c = 3.5 \times 10^6$ was used as the datum from which to develop the factor F_R applicable to the increment in maximum lift coefficient, see Section 3. Most of the data were at or around this value. The effect of Reynolds number on $\Delta C'_{L0t}$ over the ranges given in Table 5.1 and for higher Reynolds numbers can be assumed to be negligible.

The method of the Item takes no account of Mach number in the increments in maximum lift coefficient due to the deployment of high-lift devices. This is not because such effects are felt to be insignificant, since even at quite low free-stream Mach numbers the local flow around a leading-edge device can attain supersonic velocities. Rather, it is due to the lack of data for Mach numbers greater than 0.15 for the type of high-lift device considered. The use of the Item is therefore restricted to $M \leq 0.2$.

TABLE 5.1 Parameter ranges for test data for plain trailing-edge flaps used in the methods of Section 4

Parameter	*Range*
t/c	0.06 to 0.18
ρ_l/c	0.004 to 0.020
ρ_l/t	0.067 to 0.132
c_t/c	0.2 to 0.5
$\delta_t°$	–38° to + 75°
$R_c \times 10^{-6}$	2.17 to 6.0
M	0.09 to 0.15

5.2 Accuracy

Sketch 5.1 shows the comparison between predicted and experimental values of ΔC_{L0} due to the deployment of plain trailing-edge flaps. Also shown are comparisons for a plain trailing-edge flap in combination with a plain leading-edge flap. With few exceptions the predicted and test data for ΔC_{L0} are correlated within ±20%.

Similarly, Sketch 5.2 presents the corresponding values of the increment in maximum lift coefficient. Again, with few exceptions the data for ΔC_{Lm} are correlated within ±20 %.

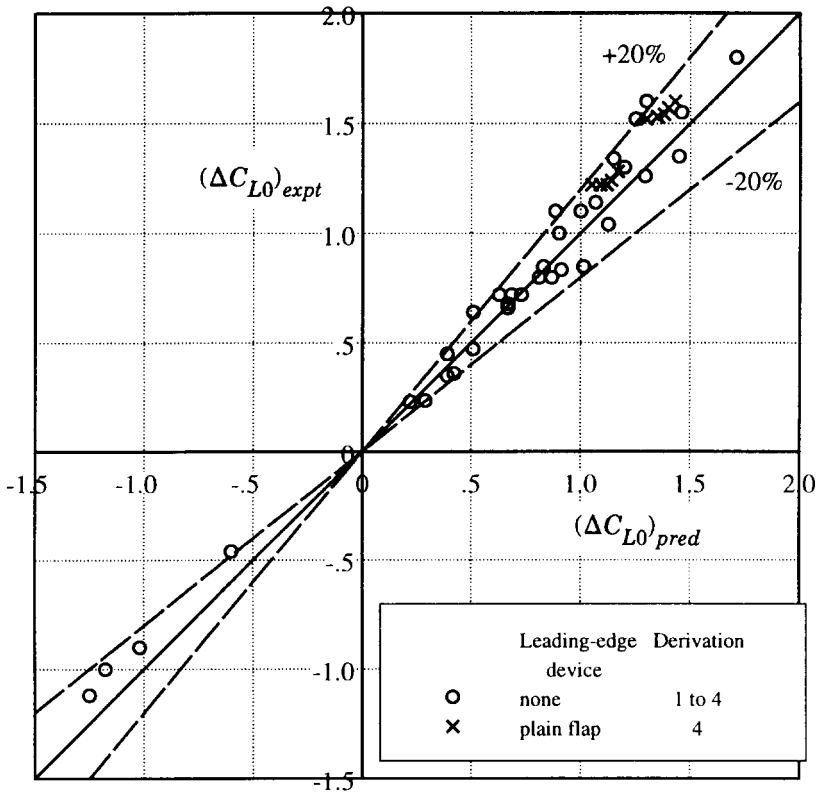

Sketch 5.1 Comparison of predicted and experimental values of ΔC_{L0}

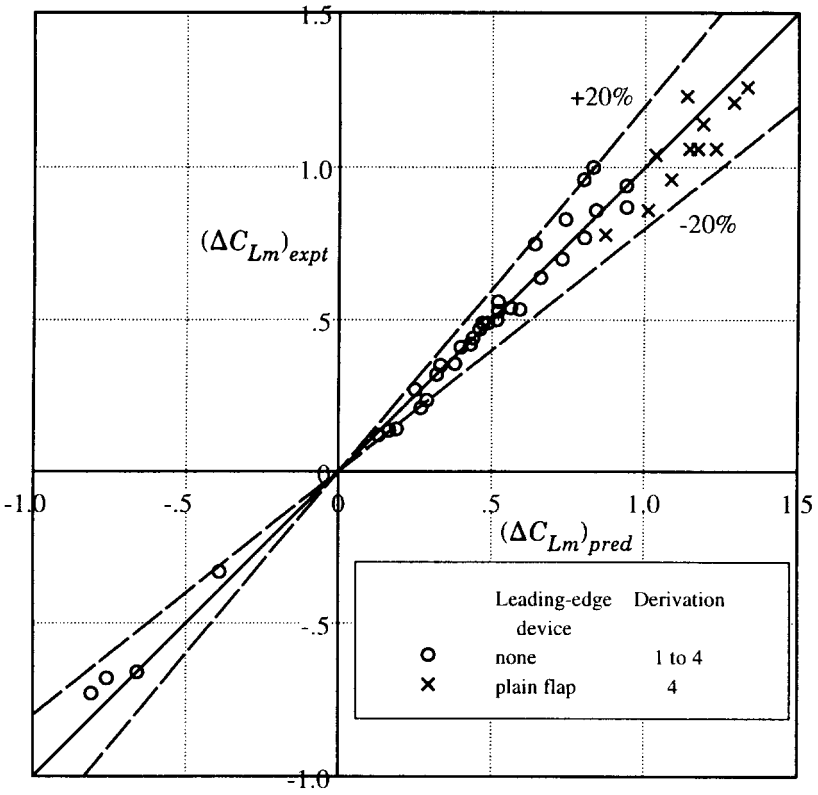

Sketch 5.2 Comparison of predicted and experimental values of ΔC_{Lm}

6. DERIVATION AND REFERENCE

6.1 Derivation

The Derivation lists selected sources of information that have assisted in the preparation of this Item.

1. WENZINGER, C.J.
   HARRIS, T.A
   Wind-tunnel investigation of an NACA 23012 airfoil with various arrangements of slotted flaps.
   NACA Rep. 664, 1938.

2. ABBOTT, I.H.
   VON DOENHOFF, A.E.
   STIVERS, L.S.
   Summary of airfoil data.
   NACA Rep. 824, 1945.

3. SPEARMAN, M.L.
   Wind-tunnel investigation of an NACA 0009 airfoil with 0.25- and 0.50-airfoil-chord plain flap independently and in combination.
   NACA tech. Note 1517, 1948.

4. GAINBUCCI, B.J.
   Section characteristics of the NACA 0006 airfoil with leading-edge and trailing-edge flaps.
   NACA tech. Note 3797, 1956.

5. THAIN, J.A.
   Reynolds number effects at low speeds on the maximum lift of two-dimensional aerofoil sections equipped with mechanical high lift devices.
   NAE (Div. Mech. Engng) *Quarterly Bulletin* No. 3, 1973.

6. SCHEMENSKY, R.T.
   Development of an empirically based computer program to predict the aerodynamic characteristics of aircraft. Volume 1: Empirical methods.
   TR-73-144 (AD 780 100), 1973.

7. BAe, Hatfield
   Unpublished wind-tunnel test data, 1985.

8. ESDU
   Increments in aerofoil lift coefficient at zero angle of attack and in maximum lift coefficient due to deployment of various leading-edge high-lift devices at low speeds.
   ESDU International, Item No. 94027, 1994.

6.2 Reference

The Reference contains information supplementary to that given in this Item

9. ESDU
   Introduction to the estimation of the lift coefficients at zero angle of attack and at maximum lift for aerofoils with high-lift devices at low speeds.
   ESDU International, Item No. 94026, 1994.

7. EXAMPLES

7.1 Example 1: Plain trailing-edge Flap

The incremental effects on the lift coefficient at zero angle of attack and on the maximum lift coefficient are to be estimated for the deployment of the plain trailing-edge flap installed on a NACA 0006 aerofoil as shown in Sketch 7.1. The relevant geometrical data are

Aerofoil	Flap
$t/c = 0.06$	$c_t = 1.35$ft
$c = 4.5$ ft	$\delta_t^\circ = 35°(\delta_t = 0.611$ rad.)
$\rho_l/c = 0.004$	
$\phi_t^\circ = 3.5°$	

The flow conditions are

$M = 0.2$ and $R_c = 4.5 \times 10^6$.

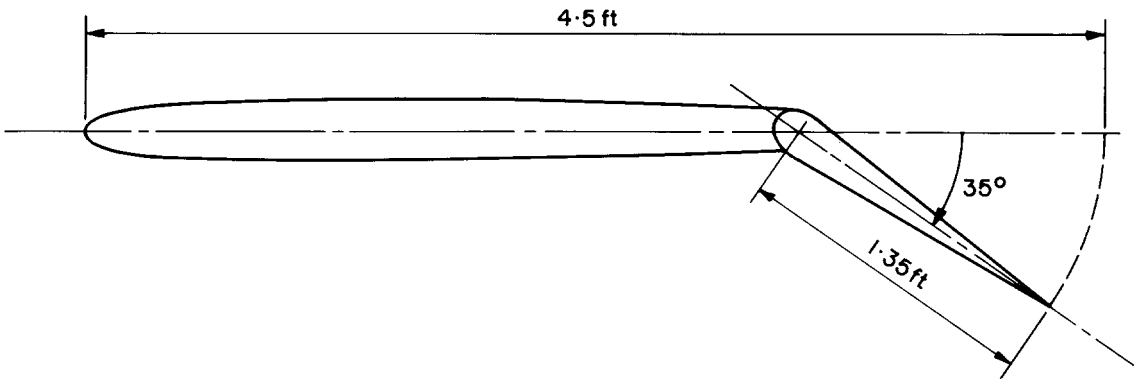

Sketch 7.1

Since the aerofoil is fitted with a plain flap the extended chord is that of the basic aerofoil, *i.e.*

$$c' = c = 4.5 \text{ ft},$$

and
$$c_t/c' = 1.35/4.5 = 0.3.$$

Calculation of ΔC_{L0t}:

for
$$\delta_t^\circ + \phi_t^\circ = 35 + 3.5 = 38.5°,$$

Figure 1 gives

$$J_P = 0.480.$$

Equation (4.5) gives $\Delta C'_{L0t}$ as

$$\begin{aligned}\Delta C'_{L0t} &= 2J_p\delta_t\{\pi - \cos^{-1}(2c_t/c' - 1) + [1-(2c_t/c'-1)^2]^{½}\} \\ &= 2\times 0.480\times 0.611\times\{\pi - \cos^{-1}(2\times 0.3 - 1) + [1-(2\times 0.3-1)^2]^{½}\} \\ &= 1.218.\end{aligned}$$

Equation (3.4) therefore gives

$$\begin{aligned}\Delta C_{L0t} &= \frac{c'}{c}\Delta C'_{L0t} \\ &= 1 \times 1.218 \\ &= 1.22.\end{aligned}$$

Calculation of ΔC_{Lmt}:

The parameter ρ_l/t is given by

$$\begin{aligned}\rho_l/t &= (\rho_l/c)/(t/c) \\ &= 0.004/0.06 \\ &= 0.0667.\end{aligned}$$

Therefore Equation (4.9) gives

$$\begin{aligned}K_G &= 1.225 + 4.525\rho_l/t \\ &= 1.225 + 4.525 \times 0.0667 \\ &= 1.527.\end{aligned}$$

Equation (4.10) gives

$$K_t = 0.8.$$

It will be assumed that separation is at the leading edge, *i.e.* $x'_s = 0$.

Thus, Figure 2 (or Equations (4.13) to (4.16)) with $c_t/c' = 0.3$ and $x'_s/c' = 0$ gives

$$T = 0.442,$$

so that Equation (4.8) gives, with the previously calculated value of $\Delta C'_{L0t}$,

$$\begin{aligned}\Delta C'_{Lmt} &= K_G K_t T \Delta C'_{L0t} \\ &= 1.527 \times 0.8 \times 0.442 \times 1.218 \\ &= 0.658.\end{aligned}$$

For $R_c = 4.5 \times 10^6$, Equation (3.3) gives

$$\begin{aligned} F_R &= 0.153 \log_{10} R_c \\ &= 0.153 \times \log_{10}(4.5 \times 10^6) \\ &= 1.018. \end{aligned}$$

Therefore, Equation (3.5) gives

$$\begin{aligned} \Delta C_{Lmt} &= F_R \frac{c'}{c} \Delta C'_{Lmt} \\ &= 1.018 \times 1 \times 0.658 \\ &= 0.67. \end{aligned}$$

Example 2: Plain Trailing-edge Flap with Drooped Leading Edge

Estimate the effects on the lift coefficient at zero angle of attack and on the maximum lift coefficient of the addition of leading-edge droop to the configuration considered in Example 1, as shown in Sketch 7.2. The relevant geometrical data for the leading-edge droop (using the notation of Item No. 94027) are

c_l = 0.675 ft
δ_l° = 20°
z_h = 0.120 ft

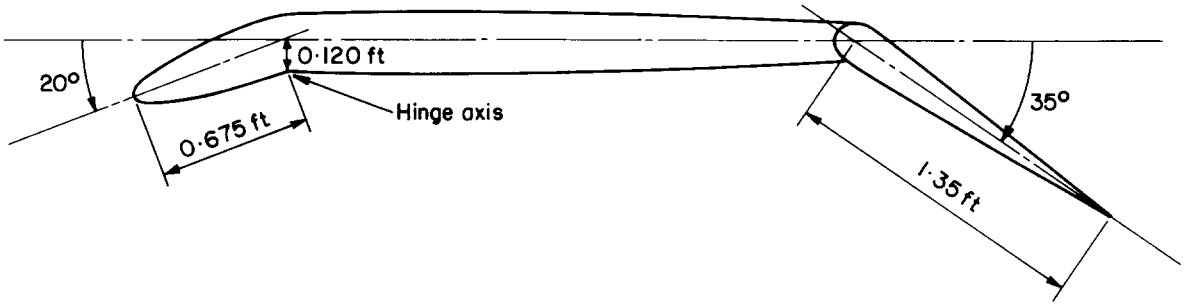

Sketch 7.2

Leading-edge Droop:

Example 1 of Item No. 94027 details the calculations for the leading-edge droop used in the present example. Reference to Section 7.1 of Item No. 94027 gives

$c' = 4.542$ ft, $c_{el}/c' = 0.153$, $c'/c = 1.009$,
$\Delta C_{L0l} = -0.059$ and $\Delta C_{Lml} = 0.423$.

These still apply when the plain trailing-edge flap is deployed.

Trailing-Edge Flap:

ΔC_{L0}:

The differences in the calculation of ΔC_{L0t} from a case in which only a trailing-edge flap is deployed relate to the revised value of c'/c with the leading-edge droop deployed. Thus, $J_p = 0.480$ as in Example 1, and so Equation (4.5) now gives, with $c_t/c' = 1.35/4.542 = 0.297$,

$$\Delta C'_{L0t} = 2J_p\delta_t\left\{\pi - \cos^{-1}(2c_t/c' - 1) + [1 - (2c_t/c' - 1)^2]^{\frac{1}{2}}\right\}$$

$$= 2 \times 0.480 \times 0.611 \times \left\{\pi - \cos^{-1}(2 \times 0.297 - 1) + [1 - (2 \times 0.297 - 1)^2]^{\frac{1}{2}}\right\}$$

$$= 1.212,$$

with which Equation (3.4) gives

$$\Delta C_{L0t} = \frac{c'}{c}\Delta C'_{L0t}$$

$$= 1.009 \times 1.212$$

$$= 1.223.$$

The total value, ΔC_{L0}, is given by equation (3.1), *i.e*

$$\Delta C_{L0} = \Delta C_{L0l} + \Delta C_{L0t}$$

$$= -0.059 + 1.223$$

$$= 1.16.$$

Comparison with Example 1 shows that the leading-edge droop deployment reduces the value of ΔC_{L0} for the configuration by 0.06, or 5%.

ΔC_{Lm}:

The differences in the calculation of ΔC_{Lmt} for the addition of leading-edge droop to the trailing-edge flap deflection arise from two sources; firstly the changed value of $c'/c(= 1.009)$ and secondly the use of $x'_s/c' = \frac{1}{2}\, c_{el}/c' = 0.153/2 = 0.077$.

The revised value of T is given by Figure 2 (or Equations (4.13) to (4.16)) with $c_t/c' = 0.297$ and $x'_s/c' = 0.077$ as

$$T = 0.389.$$

Equation (4.8) now gives, with $K_G = 1.527$, $K_t = 0.8$, $T = 0.389$ and $\Delta C'_{L0t} = 1.212$,

$$\begin{aligned}\Delta C'_{Lmt} &= K_G K_t T \Delta C'_{L0t} \\ &= 1.527 \times 0.8 \times 0.389 \times 1.212 \\ &= 0.576.\end{aligned}$$

Therefore, Equation (3.5) gives, with $F_R = 1.018$, $c'/c = 1.009$ and $\Delta C'_{Lmt} = 0.576$,

$$\begin{aligned}\Delta C_{Lmt} &= F_R \frac{c'}{c} \Delta C'_{Lmt} \\ &= 1.018 \times 1.009 \times 0.576 \\ &= 0.592.\end{aligned}$$

The total value, ΔC_{Lm}, is given by Equation (3.2), *i.e.*

$$\begin{aligned}\Delta C_{Lm} &= \Delta C_{Lml} + \Delta C_{Lmt} \\ &= 0.423 + 0.592 \\ &= 1.02.\end{aligned}$$

Comparison with Example 1 shows that the leading-edge droop deployment increases the value of ΔC_{Lm} for the configuration by 0.35, or 52%.

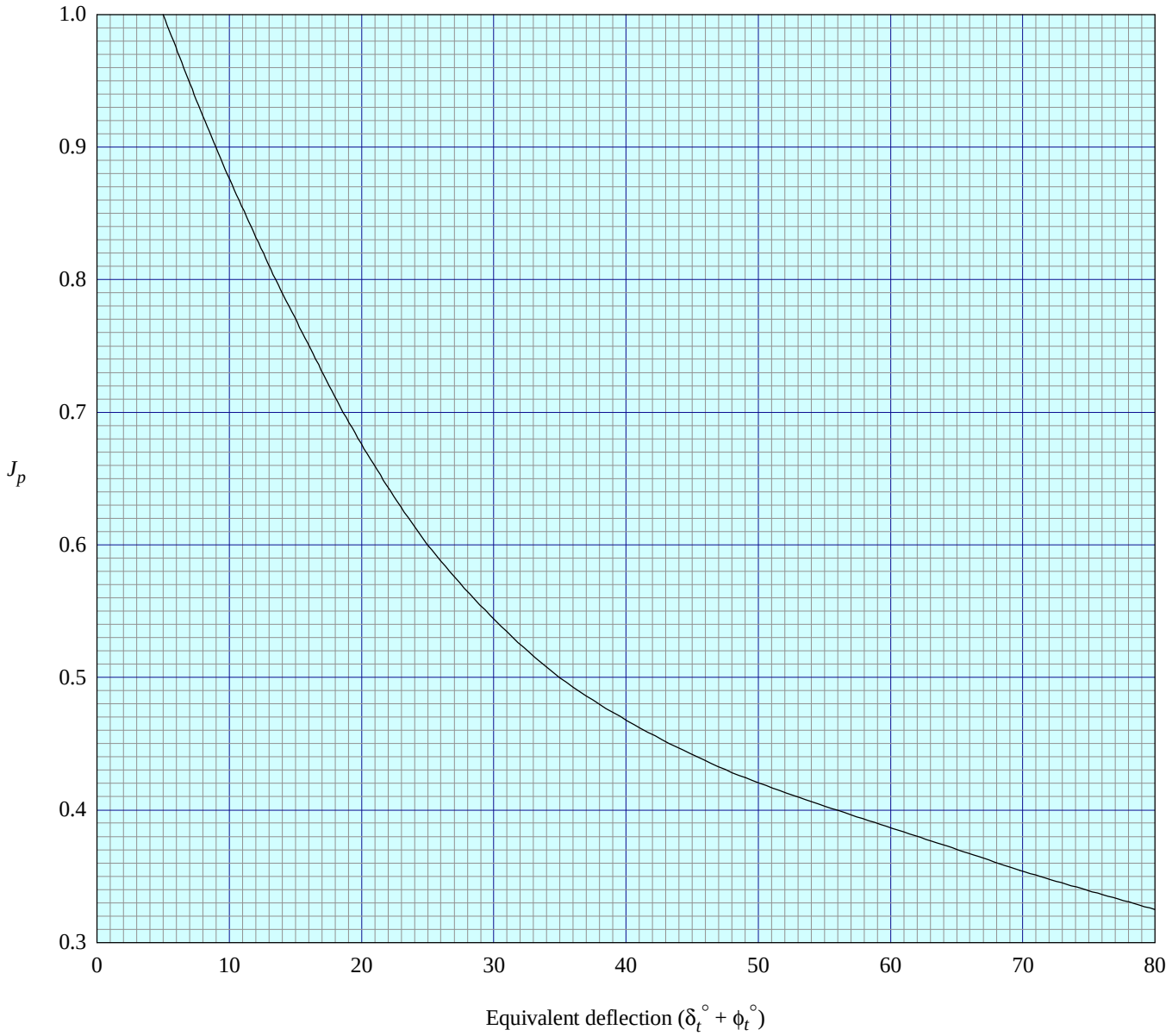

FIGURE 1 EFFICIENCY FACTOR J_p

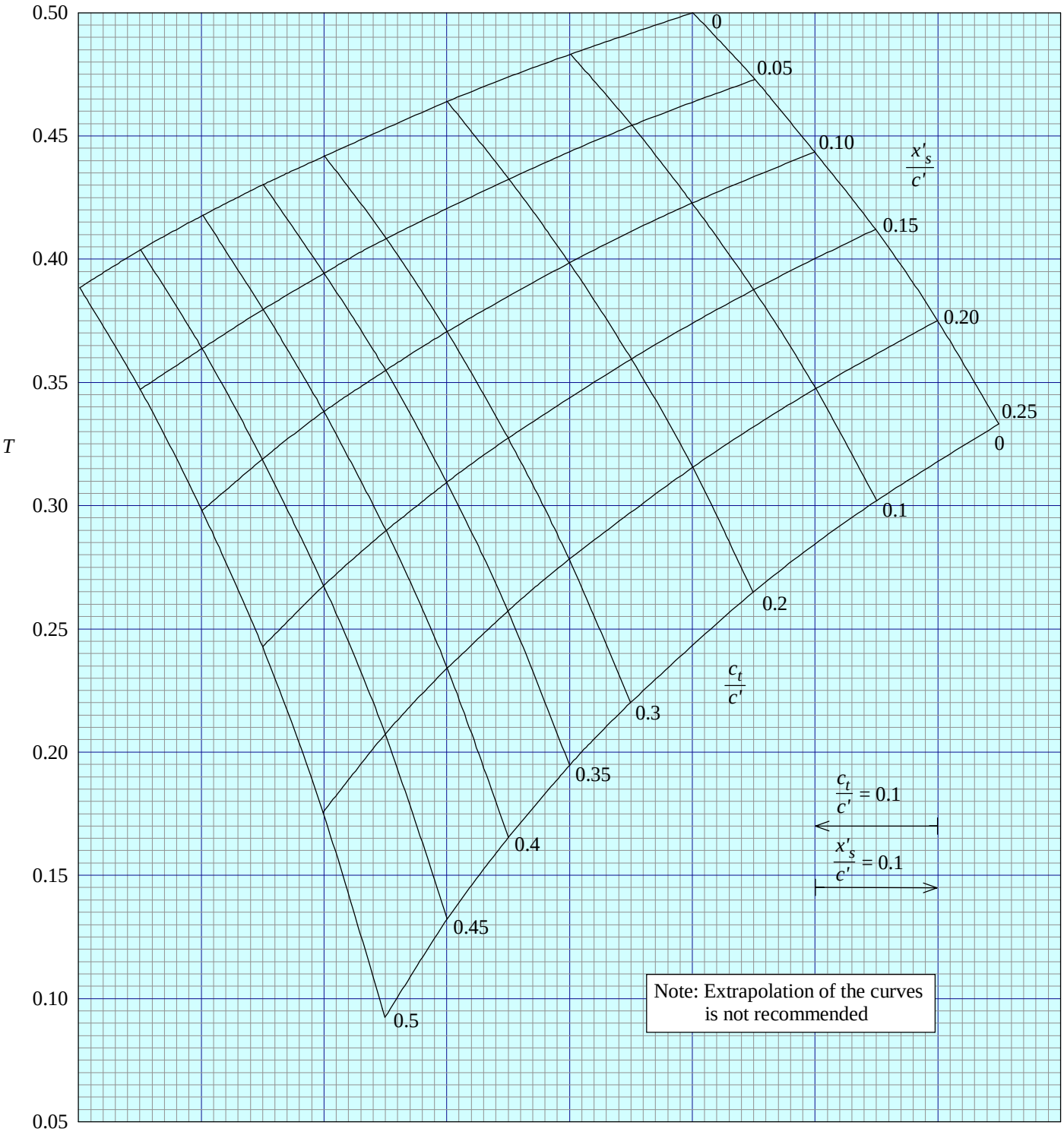

FIGURE 2 THEORETICAL PARAMETER *T*

THE PREPARATION OF THIS DATA ITEM

The work on this particular Item, which supersedes, in part, Item No. 85033, was monitored and guided by the Aerodynamics Committee which first met in 1942 and now has the following membership:

Chairman

Mr H.C. Garner	–	Independent

Members

Mr G.E. Bean*	–	Boeing Commercial Airplane Company, Seattle, Wash., USA
Dr N.T. Birch	–	Rolls-Royce plc, Derby
Mr D. Choo*	–	Northrop Corporation, Pico Rivera, Calif., USA
Dr P.C. Dexter	–	British Aerospace plc, Sowerby Research Centre, Bristol
Mr J.R.J. Dovey	–	Independent
Dr K.P. Garry	–	Cranfield University
Dr H.P. Horton	–	Queen Mary and Westfield College, University of London
Mr P.K. Jones	–	Independent
Mr R. Jordan	–	Independent
Mr K. Karling*	–	Saab-Scania, Linköping, Sweden
Mr M. Maurel	–	Aérospatiale, Toulouse, France
Mr J.B. Newton	–	British Aerospace Defence Ltd, Warton
Mr R. Sanderson	–	Deutsche Aerospace Airbus, Bremen, Germany
Mr A.E. Sewell*	–	McDonnell Douglas, Long Beach, Calif., USA
Mr M.R. Smith	–	British Aerospace Airbus Ltd, Bristol

* Corresponding Member

The technical work in the assessment of the available information and the construction and subsequent development of the Data Item was carried out under contract by Mr J.R.J. Dovey.